Optimized prediction of strain distribution with crystal plasticity supported definition of yielding direction

OPTIMIZED PREDICTION OF STRAIN DISTRIBUTION WITH CRYSTAL PLASTICITY SUPPORTED DEFINITION OF YIELDING DIRECTION

H. Hippke[1*], S. Hirsiger[1], F. Rudow[1], B. Berisha[2], P. Hora[1]

[1]Institute of Virtual Manufacturing, ETH Zurich, Tannenstrasse 3, 8092 Zurich, Switzerland
[2] inspire AG, inspire-ivp, Tannenstrasse 3, 8092 Zurich, Switzerland

ABSTRACT: The predictability of strain distributions and the related prediction of hardening and failure plays a central role in tool and process design for any metal forming process. Studying yielding behaviour it was discovered, that for various physically motivated yield loci [2,5], no satisfying agreement between DIC measured strain distribution and simulation result could be obtained, even after optimization of parameters and for both associated and non-associated flow assumption (e.g. 8 or 16 parameters). In parallel, crystal plasticity simulations were investigated with the objective to predict the relation between stress and strain ratios for a large number of load cases based on texture measurement. The resulting relations were then applied as input parameters for the plastic yield description and without further optimization almost perfect agreement between forming experiment and simulation was reached. The output can be obtained with either free shape yield loci [13,19], or non-associated flow description [15]. This publication thus presents a novel approach to use micro scale predictions of plastic yielding behaviour to calibrate macroscopic models for metals on the example of an AA6016-T4 aluminium alloy.

KEYWORDS: Yield locus, crystal plasticity, FAY, Vegter, non-associated, flow rule

1 INTRODUCTION

This contribution investigates the predictive performance of yield locus definitions. Instead of yield loci based on experimentally determined stress ratio and flow direction, it is proposed to model yield loci based on crystal plasticity prediction. Two approaches of macroscopic modelling of the CP data are compared with the industrial standard for Aluminium alloys, the YLD2000 yield locus. It becomes apparent, that a precise modelling of crystal plasticity (CP) results leads to a very detailed reproduction of strain distributions in Nakajima specimen. Both a non-associated YLD2000 and a Vegter approach lead to satisfying results.

2 STATE OF THE ART

Yield locus models for plain stress materials are under investigation recently with developments like the use of non-associated flow as suggested by Stoughton et al. [15], and higher order yield loci [1,21]. These developments extend the realm of otherwise physically motivated models, Hill'48 [5] and YLD2000 [20] and opened the discussion for mathematically motivated modelling approaches like the Vegter and FAY models. [14,19].

With the considerable yet non-exclusive list of models provided it becomes a challenge to define a measure of comparison that properly indicates the models predictability. A widely established measure is that of directional testing, usually done only for tensile conditions, to show the capability of a given model to fit measured properties for various angles to rolling direction, as shown in [11,16] for tensile stress ratios and Lankford parameter.

An evaluation of yield loci solely based on tensile properties, however, does not represent the variety of loading cases prevalent in common industrial applications. In consequence, it becomes apparent, that a larger spread of support points to other loading cases leads to a representation closer to real applications. This approach is used by the definition of hinge points in the Vegter model.

To show the predictive behaviour of yield locus models, Manopulo et al. [10] suggested a comparison with strain distributions of Nakajima testing samples focussing on the geometries B20, B100 and B200, which represent the loading conditions of tensile, plain strain and biaxial respectively. As Nakajima testing is widely available and is an integral part of material testing, this approach will be applied in this publication.

* Corresponding author: ETH Zürich Tannenstrasse 3 8092 Zürich, +41 44 633 78 09, hhippke@ethz.ch

2.1 YIELD EXPONENT

Hosford and Logan [9] suggest an exponent of 8 for FCC crystal structures and an exponent of 6 for BCC structures. With this research in mind, Hippke [6] has performed a large investigation of the order of influence of the yield exponent, showing that for different Nakajima configurations one constant exponent may not be sufficient. However, an exponent in dependency of stress state would lead to an unstable and non-continuous yield locus. To be able to increase the amount of parameters for better fitting properties, the suggested approach is a non-associated flow rule.

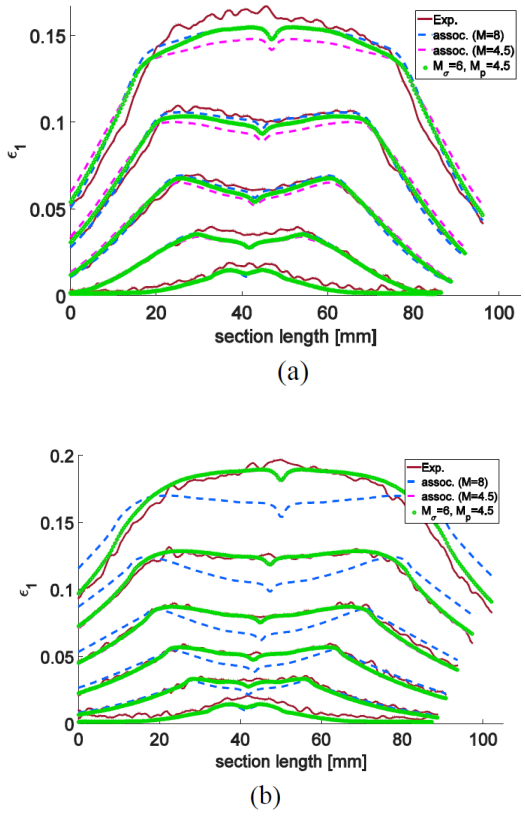

Fig. 1 *Comparison of measured and simulated major strain distributions using AFR and nonAFR approaches along the longitudinal axis of (a) B100 specimen and (b) B200 specimen* [10]

2.2 NON-ASSOCIATED FLOW

Stoughton et al. [17] have shown the opportunities provided by the use of non-associate flow rule (nonAFR) and have established a set of stability conditions to meet the physical requirement such as non-convexity and continuity. In [11] and [7] successful applications of nonAFR yield locus models are demonstrated.

As neither a change in yield exponent nor a nonAFR approach are fully satisfying, this work focuses on a new approach to define yield locus and plastic potential using the YLD2000 mathematical formulation for both, based only on predictions of crystal plasticity calculations instead of macroscopic experiments.

2.3 FREE SHAPE YIELD LOCUS – THE VEGTER MODEL

An additional model investigated within this work is the free shape yield locus model proposed by Vegter et al. [18]. The model is based on a piecewise Bézier interpolation in mayor stress space combined with a Fourier interpolation in direction of different angles to rolling direction θ. Note that this model is not defined in the plain stress space of $\bar{\sigma}=[\sigma_{xx}\ \sigma_{yy}\ \sigma_{xy}]$, but in major stress space $\bar{\sigma}_p=[\sigma_1\ \sigma_2]$. The model makes use of the transformation in (1). The definition of Bézier function based on Bernstein polynomials is given in (2) and (3) with the order n=2 and fixed points b_i. The parameter $t \in (0,1]$ indicates the position within each Bézier element. The definition of Fourier interpolation is given in (4). The assumption of orthotropic behaviour reduces the Fourier series to cos(θ) terms.

$$\bar{\sigma}=R\bar{\sigma}_p R^T \text{ with } R=\begin{bmatrix}\cos(\theta) & \sin(\theta)\\ -\sin(\theta) & \cos(\theta)\end{bmatrix} \quad (1)$$

$$b_0^n(t)=\sum_{i=0}^{n} b_i \cdot B_i^n(t) \quad (2)$$

$$B_i^n(t)=\binom{n}{i} t^i(1-n)^{n-i} \text{ with } \binom{n}{i}=\frac{n!}{i!(n-i)!} \quad (3)$$

$$f(\theta)=\varphi_0+\varphi_1\cos(2\theta)+\varphi_2\cos(4\theta) \quad (4)$$

For clarification, the concept is shown in Fig. 2.

In order to have full freedom with respect to the number of hinge points and reference points, the model was implemented as a User subroutine in the commercial FEM program LS-DYNA. The implementation follows in general the publications by Pijlman et al. [12]. The parameter set is defined in accordance with Vegter et al. [18], with one central difference. In addition to the suggested 14 parameters and a fixed plain strain stress ratio of 0.5, which corresponds to a von Mises approach, the model is extended by an input stress ratio α_{ps}. The extension increases modelling prediction for plain strain states. This extends the model to 15 parameters.

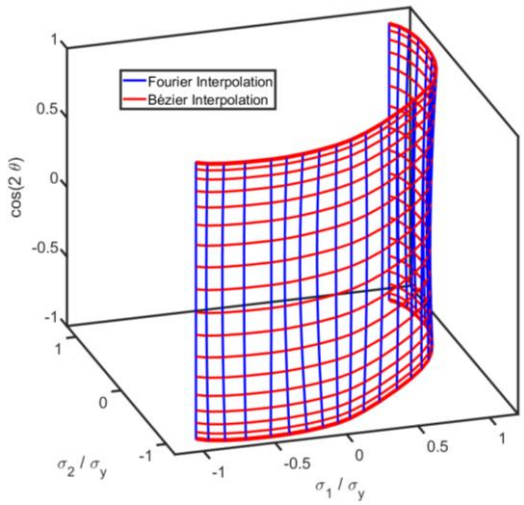

Fig. 2 *Concept of the Vegter model based on both Bézier and Fourrier interpolation.*

3 DETERMINISTIC CRYSTAL PLASTICITY APPROACH

After X-Ray measurements of the grain orientations of an AA6014-T4 aluminium alloy, crystal plasticity calculations with 50 representative orientations have been performed in the CP-FFT program DAMASK checking different loading paths in stress space to evaluate the yield points and flow directions [3,8].

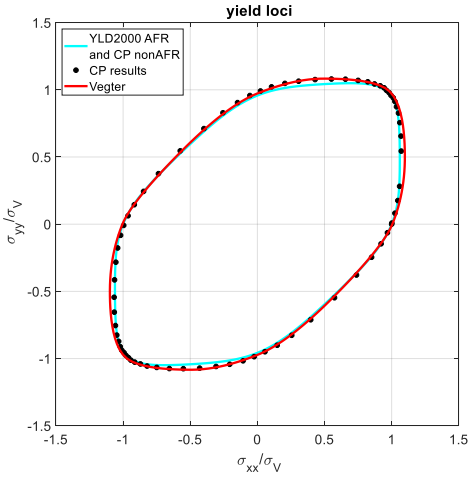

Fig. 3 *CP result in stress space and yield loci of all models considered.*

3.1 YIELD LOCUS FROM CP

Hirsiger and Berisha [3,8] have presented the computed yield locus of the AA6016-T4 aluminum alloy. The RVE contains 16^3 FFT points and therefore, app. 80 points per grain are considered. The yield points are taken at 4% equivalent plastic strain.

3.2 YIELDING DIRECTION FROM CP

In the framework of RVE computations the deformation gradient $\boldsymbol{F}$ can be prescribed at the boundaries of the RVE and an iterative procedure is necessary to find the equilibrium of the stresses. In the context of yield locus computation linear strain paths are prescribed and therefore, the total strain tensor can be computed as

$$\boldsymbol{\varepsilon} = ln\boldsymbol{V} \tag{5}$$

where $\boldsymbol{V}$ is the left stretch tensor computed from the polar decomposition of the deformation gradient $\boldsymbol{F} = \boldsymbol{VR}$. In [4] the strain ratios have been computed and the results are shown in Fig 4. This data are used to fit the parameters of the YLD200-2d potential of the nonAFR.

4 MACROSCOPIC MODELLING OF CP RESULTS

The initial approach was to fit both yield point and derivative results of the crystal plasticity calculation with an associated YLD2000 modelling approach. The result can be seen in Fig. 3. This approach returns almost perfect correlation for the yield points but a non-satisfying correlation for the derivatives. Compare fitting results of derivatives in Fig. 4. In consequence, more advanced modelling approaches are investigated.

The material parameters needed for the basic macroscopic fitting of yield curve and yield locus are determined by tensile and bulge testing. The resulting material parameters and the corresponding fitted parameters of all models are shown in Table 1: and Table 2: respectively.

4.1 NON-ASSOCIATED APPROACH

The first advanced modelling strategy chosen is a nonAFR YLD2000 approach to model the yield points and the derivatives as calculated with CP separately. To show the impact of the derivative, the yield locus is chosen identical to the AFR approach and only the plastic potential is fitted to the CP data using the YLD2000 mathematical formulation. This reproduces the predicted behaviour correctly, as shown in Fig. 3 and Fig. 4. This approach shows almost perfect correlation with the CP data points, see CP nonAFR in all figures. The exponent of the potential is included as parameter in the optimization and is returned as 5.1.

It is remarkable that two of the potential parameters are optimized to be 1.0. This may indicate, that not the full parameter set is needed for an optimized fitting, however it may also indicate that the input parameters are not sufficient to force the optimizer to make use of every parameter.

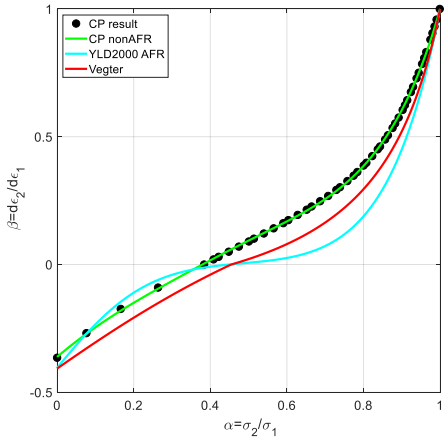

Fig. 4 *Strain directions as β(α) from CP and result of all models considered.*

Table 1: *Measured material parameters and Hockett-Sherby yield curve fit for AA6016-T4*

σ_0 [MPa]	σ_{45} [MPa]	σ_{90} [MPa]	σ_b [MPa]
123.7	119.35	120.27	122.02
R_0	R_{45}	R_{90}	R_b
0.6870	0.5005	0.6668	1.0
A [MPa]	B [MPa]	m	n
352.4	123.7	5.62	0.865

Table 2: *Parameters of fitted yield locus models*

YLD2000 AFR	α_1	α_2	α_3	α_4
	0.9292	1.0514	0.9594	1.0438
	α_5	α_6	α_7	α_8
	1.0277	1.0364	0.9683	1.1554
CP potential	α_1	α_2	α_3	α_4
	1.6814	0.0009	0.2922	1.2354
	α_5	α_6	α_7	α_8
	1.0745	1.5672	1.000	1.000
Vegter	f_{ps00}	f_{ps45}	f_{ps90}	f_{bi}
	1.0985	1.0675	1.0832	0.9868
	f_{un00}	f_{un45}	f_{un90}	ρ_{bi00}
	1.005	0.9650	0.9728	0.9996
	f_{sh00}	f_{sh45}	f_{sh90}	α_{ps}
	0.5542	0.5617	0.5542	0.4545
	R_0	R_{45}	R_{90}	
	0.6870	0.5005	0.6668	

4.2 ASSOCIATED APPROACH WITH HIGHER ORDER YIELD LOCI

The second approach tested is the representation of flow behaviour with the Vegter model, as described in chapter 2.3, once more the modelling result is shown in Fig. 3 and Fig. 4.

The selection of reference points in this publication is in accordance with the original suggestion by Vegter. In consequence, both stress point and derivative are defined at tensile, shear, plain strain and biaxial tension in rolling direction, diagonal direction and transverse direction. Derivatives and yield points are extracted from CP data with exception of the tensile data points, where experimentally measured stress ratios and R-values are used.

5 PREDICTION OF STRAIN DISTRIBUTION

To validate the model predictability for a process close to metal forming applications, strain distributions extracted from Nakajima testing samples are selected. As reference configurations, the samples B20, B100 and B200 are selected as they represent tensile, plain strain and biaxial loading conditions. Measurements of both major and minor strain distribution via DIC (GOM ARAMIS) are compared with simulation results at identical drawing depth.

5.1 EXPERIMENTAL MEASUREMENT OF NAKAJIMA STRAIN DISTRIBUTION

The experimentally measured major strain determined from DIC measurement is shown in Fig. 5 and the minor strain is shown in Fig. 6 for all three Nakajima configurations considered. Since this publication is focussing on prediction of plastic behaviour rather than failure, drawing depths with apparent localization are omitted.

5.2 EVALUATION OF MODEL PREDICTION

For the evaluation of the different models calculations in LS-DYNA R11 were performed. The material model subroutine uses an explicit return-mapping algorithm to calculate the yield stress and the general FEM is integrated explicitly with selective mass scaling at a time step of 1.e-7. The friction is assumed to be insignificant between punch and sheet. For all other contact surfaces a friction coefficient of μ=0.1 is used.

The non-associated CP-based YLD2000 model predicts the strain distribution for all three specimen almost perfectly. However, the Vegter model shows greater agreement for the tensile and plain strain specimen and only under predicts the strain for the biaxial configuration.

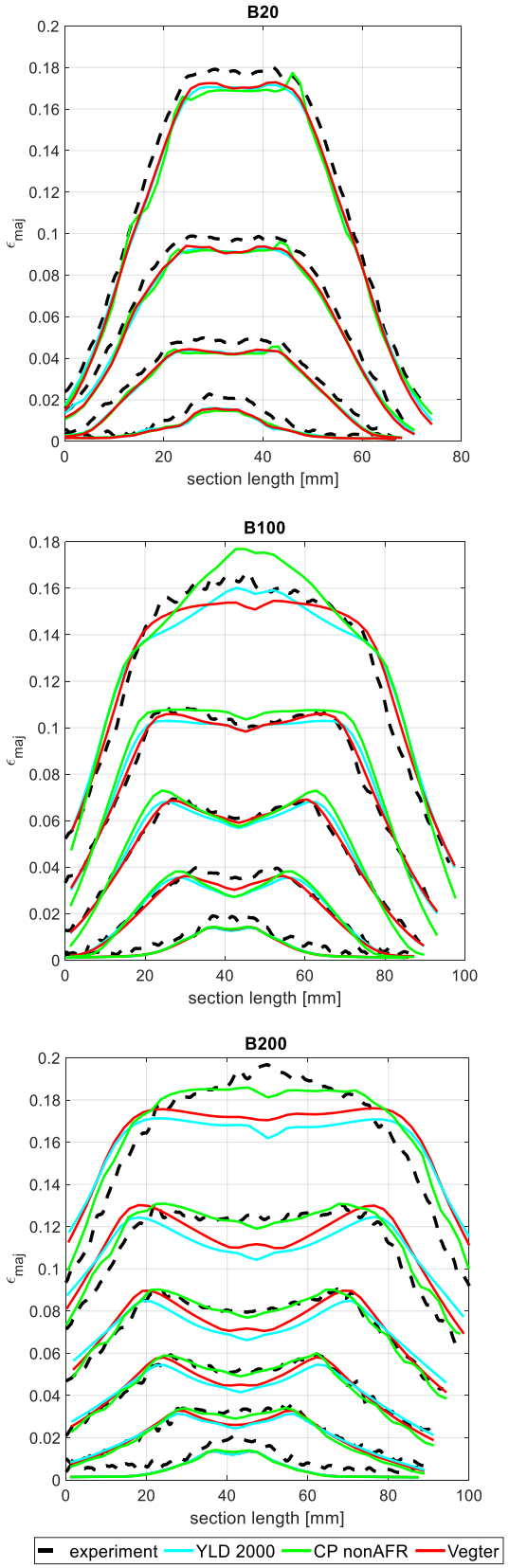

Fig. 5 *Measured major strain distribution and model predictions for configurations a) B20, b) B100 and c) B200.*

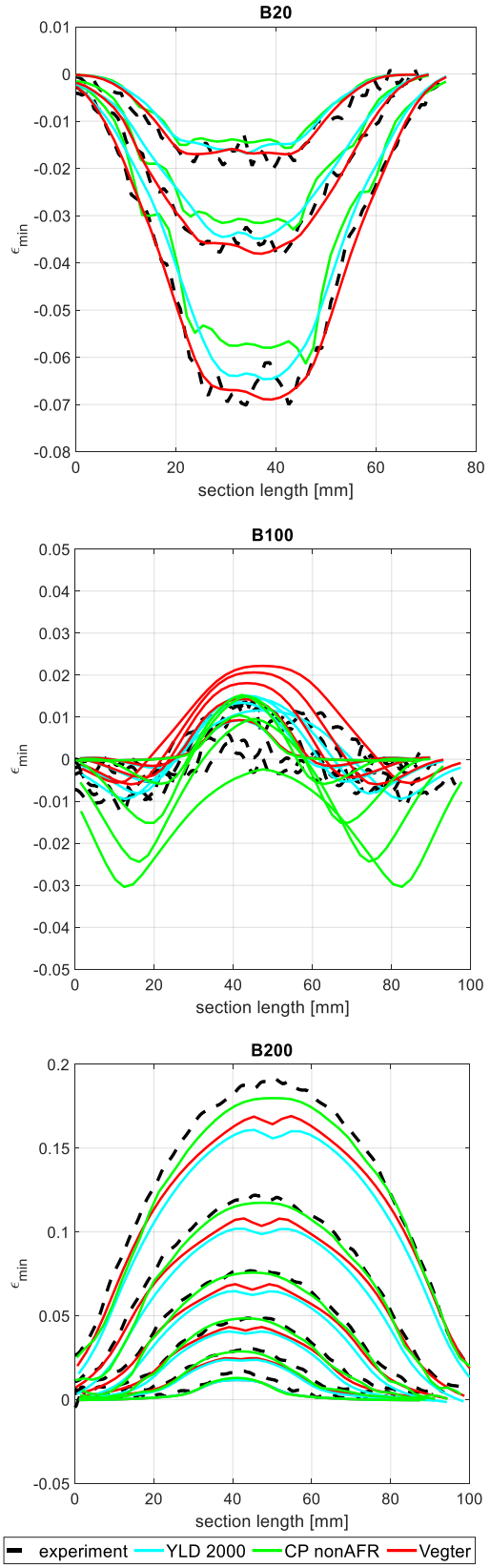

Fig. 6 *Measured minor strain distribution and model predictions for configurations a) B20, b) B100 and c) B200.*

6 CONCLUSION

Calculating stress ratios and flow direction based on a texture measurement with a crystal plasticity software is able to predict the yielding behaviour of the presented Aluminium alloy at higher precision than models commonly used. Additionally this approach his able to reduce the number of experiments needed to a minimum. The only downside is an increased computational cost.

Currently, crystal plasticity calculations only provide individual data points and not a continuous model. In consequence, a macroscopic fit is still needed for applications in FEM.

While the nonAFR YLD2000 fit performed perfectly in this study, it needs to be stated that the plastic potential has a tendency of overfitting as the $\beta(\alpha)$ values predicted only cover the area of half the first quadrant (0° tensile-tensile range).

The performance of the mathematically based yield locus model by Vegter was also very good considering not all suggested experiments were conducted. Additionally, the model has the intrinsic flexibility to be divided into a larger number of Bézier elements, which would further increase precision. A combination of CP prediction with a high-resolution Vegter yield locus will be a focus of future work.

REFERENCES

[1] Abspoel M, Scholting ME, Lansbergen M, Neelis BM. *Accurate anisotropic material modelling using only tensile tests for hot and cold forming*. J Phys Conf Ser 2017; 896:3–10.

[2] Barlat F, Brem JC, Yoon JW, Chung K, Dick RE, Lege DJ, Pourboghrat F, Choi S-H, Chu E. *Plane stress yield function for aluminum alloy sheets - part 1: theory*. Int J Plast 2003; 19:1297–1319.

[3] Berisha B, Hirsiger S, Hippke H, Hora P. *Modeling Of Anisotropic Hardening And Grain Size Effects Based On Advanced Crystal Plastictiy Models* 41st Solid Mechanics Conference 2018; 1:2–3.

[4] Berisha B, Hirsiger S, Hora P. *CP-RVE Based AFR/NAFR Concepts*. Internal Report IVP, ETH. 2018.

[5] Hill R. *A theory of the yielding and plastic flow of anisotropic metals*. Proc R Soc London Ser A Math Phys Sci 1948.

[6] Hippke H. *Analysis Of Advanced Material Models For Complex Industrial Forming Processes*. Master Thesis ETH, 2016.

[7] Hippke H, Manopulo N, Yoon JW, Hora P. *On the efficiency and accuracy of stress integration algorithms for constitutive models based on non-associated flow rule*. Int J Mater Form 2017.

[8] Hirsiger S, Berisha B, Raemy C, Hora P. *On the prediction of yield loci based on crystal plasticity models and the spectral solver framework.* Journal of Physics: Conference Series. 2018.

[9] Logan RW, Hosford WF. *Upper-bound anisotropic yield locus calculations assuming 〈111〉-pencil glide*. Int J Mech Sci 1980; 22:419–430.

[10] Manopulo N, List J, Gorji M, Hora P. *a Non-Associated Flow Rule Based Yld2000-2D Model*, 6016.

[11] Park T, Chung K. *Non-associated flow rule with symmetric stiffness modulus for isotropic-kinematic hardening and its application for earing in circular cup drawing*. Int J Solids Struct 2012; 49:3582–3593.

[12] Pijlman HH, Huetink J, Carleer BD, Vegter H. *Application of the Vegter yield criterion and a physically based hardening rule on simulation of sheet forming* 1998:763–768.

[13] Raemy C, Manopulo N, Hora P. *A Fourier series based generalized yield surface description for the efficient modelling of orthotropic sheet metals*. J Phys Conf Ser 2017; 896.

[14] Raemy C, Manopulo N, Hora P. *A generalized anisotropic and asymmetric yield criterion with adjustable complexity*. Comptes Rendus - Mec 2018.

[15] Stoughton TB. *A non-associated flow rule for sheet metal forming.* International Journal of Plasticity. 2002.

[16] Stoughton TB, Yoon JW. *Paradigm change: Alternate approaches to constitutive and necking models for sheet metal forming*. AIP Conf Proc 2011; 1383:15–34.

[17] Stoughton TB, Yoon JW. *On the existence of indeterminate solutions to the equations of motion under non-associated flow*. Int J Plast 2008; 24:583–613.

[18] Vegter H, Van Den Boogaard AH. *A plane stress yield function for anisotropic sheet material by interpolation of biaxial stress states*. Int J Plast 2006.

[19] Vegter H, ten Horn C, Abspoel M. *The Corus-Vegter Lite material model: Simplifying advanced material modelling*. Int J Mater Form 2009; 2:511–514.

[20] Yoon J-W, Barlat F, Dick RE, Chung K, Kang TJ. *Plane stress yield function for aluminum alloy sheets part II: FE formulation and its implementation*. Int J Plast 2004; 20:495–522.

[21] Yoon JW, Barlat F, Dick RE, Karabin ME. *Prediction of six or eight ears in a drawn cup based on a new anisotropic yield function*. Int J Plast 2006.